

Heterogeneous Manifestations of Four Cases with Erdheim-Chester Disease by Nuclear Medicine Imaging Modalities: Case Report

Erdheim Chester Hastalığı Olan Dört Olgunun Nükleer Tıp Görüntüleme Yöntemlerindeki Heterojen Bulguları

Ümmühan ABDÜLREZZAK,^a
Serap DOĞAN,^b
Mustafa KULA,^a
Elif KOCAĞAOĞLU,^a
Yurdagül KÖSE KURT,^a
Ahmet TUTUŞ^a

Departments of
^aNuclear Medicine,
^bRadiology,
Erciyes University Faculty of Medicine,
Kayseri

Geliş Tarihi/Received: 12.12.2015
Kabul Tarihi/Accepted: 09.05.2016

Yazışma Adresi/Correspondence:
Ümmühan ABDÜLREZZAK
Erciyes University Faculty of Medicine,
Department of Nuclear Medicine,
Kayseri,
TÜRKİYE/TURKEY
ummuhan@erciyes.edu.tr

ABSTRACT Erdheim–Chester disease (ECD) is an uncommon, sporadic, non-Langerhans cell histiocytosis characterized by xanthomatous or xanthogranulomatous histiocyte infiltration of affecting both bone and soft tissue systems. Herein we report the imaging features of four cases of ECD who had different multiorgan manifestations. The nuclear medicine imaging modalities consisting of technetium-99m methylene-diphosphonate (Tc-99m MDP) scintigraphy, Fluorine-18 2-deoxy-2-fluoro-D-glucose positron emission tomography/computed tomography (F-18 FDG PET/CT) and Ga-68 DOTA-octreotate (DOTA-TATE) PET/CT are useful methods to determine the ordinarily and extraordinarily heterogeneous clinical manifestations of ECD.

Key Words: Erdheim–chester disease; technetium tc 99m (sn)methylenediphosphonate; fluorodeoxyglucose f18; 68ga-dotatate

ÖZET Erdheim-Chester Hastalığı (ECH) nadir görülen, sporadik, hem kemik hem de yumuşak doku sistemlerini etkileyen ksantomatoz veya ksanto-granüloamatöz histiyosit infiltrasyonu ile karakterize Langerhans hücreli olmayan histiyositozlardandır. Bu yazıda farklı organ tutulumları olan dört ECH olgusunun görüntüleme bulguları sunulmaktadır. Teknesyum-99m methylene-diphosphonate (Tc-99m MDP) sintigrafisi, Flor-18 florodeoksiglukoz pozitron emisyon tomografisi/ bilgisayarlı tomografi (F-18 FDG PET/CT) ve Ga-68 DOTA-octreotate (DOTA-TATE) PET/CT gibi nükleer tıp görüntüleme modaliteleri ECH'nın alışılmış ve alışılmış olmayan farklı klinik manifestasyonlarını göstermede faydalı metodlardır.

Anahtar Kelimeler: Erdheim–chester hastalığı; teknesyum tc 99m (sn)metilendifosfonat; florodeoksiglukoz f18; 68ga-dotatate

Türkiye Klinikleri J Med Sci 2016;36(2):111-8

Erdheim-Chester disease was first described in 1930 as a granulomatous lipoidosis by Jacob Erdheim and William Chester.^{1,2} The disease, a rare non-Langerhans cell histiocytosis, is characterized by symmetrical involvement of the long bones with distinctive radiological and nuclear medicine imaging. Due to its rarity, a high level of clinical suspicion is required to make this laborious diagnosis because many doctors have not encountered it before. Besides bone findings, in up to 60% of cases, various organ deficits related to histiocytic infiltration can occur in this progressive disease. The disease primarily affects adults between 50-70 years old, but it can occur at all ages.³⁻⁵ There is no known cause. The characteristic clinical

presentations can be found in the skeletal system, nervous system, eyes, pulmonary system, lymphoid and hematological system and heart.⁶⁻¹¹

The clinical course depends on the particular sites or organs affected and the severity of involvement. The multi systemic form of ECD, particularly in those with central nervous system or cardiac involvement, is associated with noticeably poor prognosis.¹⁰⁻¹² Although the diagnosis of ECD is based on tissue or bone biopsies that show proliferation of histiocytes, knowing where a proper biopsy sample should be taken from is generally difficult. Nuclear medicine imaging modalities offer a complete assessment of the extent of the disease, which is important to help guide the treatment plan.

The ^{99m}technetium-methylene diphosphonate (^{99m}Tc-MDP) bone scan is useful in showing the sites of pathognomonic involvement in the skeleton.¹³ The characteristic pattern of symmetrical increased tracer uptake particularly in the metaphyso-diaphyseal regions of the long bones, and sometimes in the axial skeleton and through the mandible should be considered in the diagnosis of ECD. However, because of the difficulties of an osteomedullary or bone biopsy, to determine an easier biopsy site, extensive evaluation of all ECD patients should be performed with fluorodeoxyglucose positron emission tomography/computed tomography (FDG PET/CT), which also provides evaluation of soft tissues and bone marrow separately. Because activated inflammatory cells demonstrate increased expression of glucose transporters, FDG PET/CT has an advantage over the other imaging modalities in ECD in those with multi systemic involvement, while also offering a global assessment of all the lesions during a single session.^{14,15} There are several cases in the literature reporting that while Ga-67 citrate scintigraphy reveals a similar accumulation with the ^{99m}Tc-MDP bone scan, it offers some additional information about extra osseous involvement.^{16,17} However, to date Ga-68 labeled somatostatin receptor analog imaging of ECD has not been reported yet. In this article, we present the nuclear medicine imaging features of four cases with ECD which showed heterogeneous manifestations.

CASE REPORTS

CASE 1

A 63-year-old male presented with central diabetes insipidus, hypogonadism, extensive bone pain, headache, and loss of weight for the past 2 months. A medical history and physical examination revealed periorbital edema, visual impairment and bilateral upper and lower extremity tenderness. The patient was referred to the nuclear medicine department for a whole body bone scan to examine the cause or location of common bone pain. The Tc-99m MDP bone scan (Figure 1) showed increased tracer uptake in long bones, maxillary and mandible. The gadolinium-enhanced brain magnetic resonance imaging (MRI) revealed a well defined, lobulated, 23 x 14 mm in diameter pituitary gland lesion in the sellar region. An excisional biopsy of the pituitary lesion was performed. A section cut from the paraffin blocks of the pituitary lesion revealed non granulomatous histiocyte rich cells with entrenched lymphocytes. Various histiocytes had an expansive foamy cytoplasm with the presence of attending broad fibrillary glial tissue. The patient was referred to the department of nuclear medicine for Fluorine-

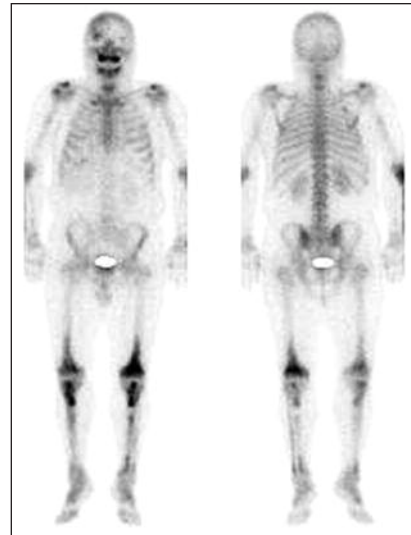


FIGURE 1: In a 63-year-old male patient, the Tc-99m MDP bone scan showed symmetric increased tracer uptake in the distal metaphyseal-diaphyseal region of both femurs, proximal and distal metaphyseal-diaphyseal region of both tibias and humeri, radii, and wrist, spreading the epiphyseal lines. The maxillary and mandible bones revealed markedly increased uptake.

18 fluorodeoxyglucose (F-18 FDG) PET/CT to determine the metabolic activity of the pituitary and bone lesions and whether or not there was other tissue involvement (Figure 2). Then, Ga-68 DOTA-TATE imaging was performed in the patient to determine whether the lesions showed expression of somatostatin receptor and to guide further management (Figure 3). By reason of the Ga-68 DOTA-TATE scan, it was decided that the patient was not a good candidate for various forms of treatment like peptide receptor radionuclide therapy.

The paraffin blocks of the pituitary gland lesion resected surgically were analyzed using the BRAF (V600E) mutant-specific antibody to determine the BRAF mutation for treatment planning. The heterozygote V600E mutation was detected in the BRAF exon 15 by DNA sequencing using PCR amplification.

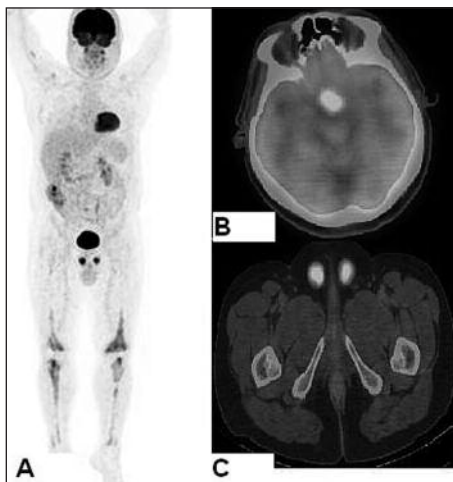


FIGURE 2: F-18 FDG-PET/CT scan (A) showed involvement of various organ systems in a 63-year-old male patient with Erdheim-Chester disease (Case 1). (B) Remarkable abnormal 18F-FDG accumulation (SUV max: 36.6) was seen in the sellar region. High FDG uptake (SUV max: 8.7) was observed in the right and left areas of the maxillary bone and at the level of the roots of the molar teeth of the mandibular bone. Moderately and intensely increased tracer accumulation (SUV max: 11.0) associated with cortical and intramedullary sclerosis was noted in the bilateral proximal humeri, scapular glenoid, distal metaphyseal-diaphyseal region of the femur, along the bilateral tibiae, predominantly on the left side, in the distal shaft of the right fibula and mid and distal region of the left fibula. Mild and moderate FDG uptake (SUV max: 6.8) was observed in the 5th cervical, 6th thoracic and 5th lumbar vertebral bodies. In addition, an intense diffuse uptake (SUV max: 16.9) was observed appertaining to bilaterally testicular parenchyma related to the disease involvement (C). F-18 FDG uptake was also viewed intensively within a circumferential region of 15 mm diameter in the cecal wall (SUV max: 21.8) considered to belong to soft tissue mass.



FIGURE 3: Maximum-intensity-projection (MIP) image of Ga-68 DOTA-TATE PET/CT in the first patient with Erdheim-Chester disease (Case 1). A, The pituitary lesion showed moderate uptake on Ga-68 DOTA-TATE PET/CT not clearly identified from physiological uptake. The colonic lesion and testicular parenchymas were negative for uptake of Ga-68 DOTA-TATE, whereas in the skeletal system, bone and bone marrow lesions reveal mild and moderate uptake with an SUV max of 5.4.

Testicular biopsy confirmed foamy histiocyte infiltration due to ECD with positivity of CD68 and CD163 and negativity of CD1A and S100 in the immunohistochemical staining.

Endoscopic biopsy taken from the cecal lesion showed a tubular adenoma without dysplasia.

CASE 2

A 40-year-old male with a history of left intertrochanteric hip fracture and prosthesis surgery 8 years previously presented with occasional bone pain in the left hip, and bilaterally in the knees and feet. A bone marrow biopsy taken from the right distal femur showed myelofibrosis with hypocellularity. MR depicted osteonecrosis and bone infection with reactive changes in the bone and soft tissue in addition to patchy bone marrow sclerosis and edema. Subsequently, bone scintigraphy was performed to identify the regions of bone involvement (Figure 4). Bone scan findings were suggestive of bone involvement compatible with a systemic disease. The bone marrow biopsy repeated according to bone scan illustrated that there were infiltrations consisting of foamy histiocytes within the bone trabeculae. Due to the possibility of involvement of various organs and

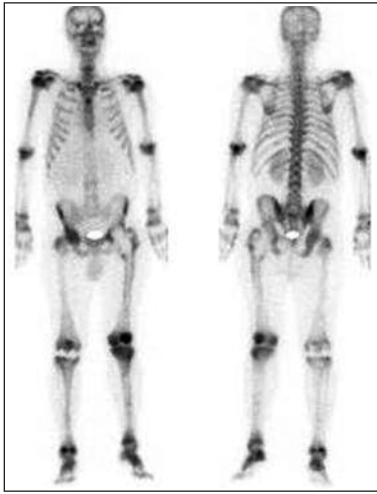


FIGURE 4: Tc-99m MDP scintigraphy of a 40-year-old male patient showed increased radiotracer uptake in the bilateral humeri, elbow, and wrist, in the bilateral scapular glenoid, distal metaphyseal-diaphyseal region of the femur, proximal and distal metaphyseal-diaphyseal region of the tibiae, and in the tarsal bones of the feet.

tissues, and to monitor whole body metabolic activity, F-18 FDG PET/CT was performed in the patient (Figure 5).

CASE 3

A 14-year-old male presented with febrile episodes (38°C) and arthromyalgia, especially in the knees. Blood tests did not show any abnormality. Due to increasing bone pains two months later, the radiographs taken of his legs and thighs showed bilateral patchy intramedullary sclerosis of the shafts and metaphyseal portions of the bilateral femurs, and tibiae, and bilateral fibulae. MR images of the legs showed, in addition to muscle edema, decreased marrow signal intensity on T1-weighted images and increased signal intensity on T2-weighted images in the bilateral proximal metaphyseal regions of the tibiae. Initially, as a result of these clinical and radiological features, the patient was thought to have an infection and the analysis of the pathology specimen of the bone supported chronic multifocal osteomyelitis.

Despite long term antibiotic therapy, the patient did not respond clinically to the treatment, and underwent the bone scan to monitor the results. The whole body bone scan (Figure 6) was performed. The clinical data, involvement and dis-

tribution patterns of the bone scan findings suggested a certain form of Non-Langerhans' cell histiocytosis called ECD. Therefore, as a result of reviewing and immunohistochemical staining the previously obtained bone specimen, the diagnosis of ECD was validated by pathologists.

CASE 4

A 40-year-old woman was admitted to the hospital complaining of a three-month history of dizziness, cotton mouth, polydipsia, polyuria and knee pain. Because of the persistent oral mucosal infection, she had previously been evaluated at another institution and had been treated with antibiotics and acetaminophen. As the sore lesions in the mouth did not heal for two weeks, an incisional biopsy was carried out on the oral mucosa. Histopathological investigation of the mucosal lesion revealed lymphocytic and eosinophilic infiltration organizing with enhanced cytoplasm and loose chromatin structure, obscuring the papillary epidermis. Brain

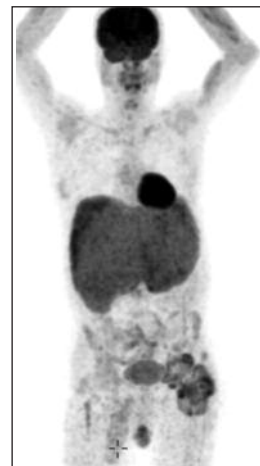


FIGURE 5: F-18 FDG-PET/CT scan showing involvement of various organ systems in a 40-year-old male patient with Erdheim-Chester disease (Case 2). The liver was so large that it filled the splenic area on the left and reached up to the level of pelvic entrance on the right. Non-uniform areas of increased FDG uptake (SUV max:8.1) not clearly outlining the contour in the subcapsular regions of the liver were seen especially on the right lobe. The spleen was not visualized. In the mediastinal and abdominal regions, multiple enlarged lymph nodes revealed a mild and moderately increased FDG uptake (SUV max:3.2). In the peripheral region of the left hip prosthesis, intense FDG uptake (SUV max:8.0) was seen belonging to the soft tissue lesion and this spread to the surrounding muscle tissues. In the proximal diaphysis, lengthening of up to 8 cm of the right femur, and moderate FDG uptake (SUV max:3.6) were observed relating to the intramedullary hyperdense lesion accompanied by calcifications.

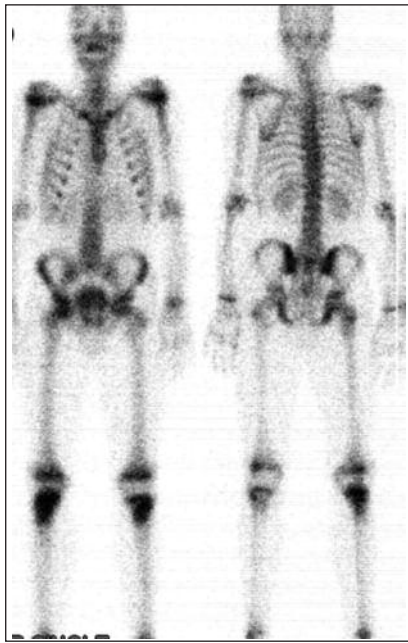


FIGURE 6: A 14-year-old male with a history of bone infection (Case 3). The follow-up Tc-99m MDP whole body bone scan revealed the corticomedullary involvement in both upper and lower extremities, especially in the metaphyseal-diaphyseal portions of the long bones; typical for Erdheim-Chester disease.

magnetic resonance imaging showed a thickening of 3.6 mm in the proximal portion of the pituitary stalk. The thickened portion of the stalk revealed diffuse contrast enhancement. The width of the sellar cavity was normal. Bone scintigraphy with Tc-99m MDP was performed (Figure 7). Clinico-pathological findings and symmetrical involvement of the long bones in imaging methods were typical for ECD.

DISCUSSION

Although the clinical spectrum shows a broad variation, ECD predominantly tends toward typical bone findings in the literature and its characteristic imaging findings takes place generally in the front of the histopathological diagnosis.¹⁸ Because it is a rare disease, a consensus definition has not yet been reached about the other collaborative soft tissue findings of the disease. Compared to conventional CT imaging or X-ray, nuclear medicine imaging methods, such as whole body bone scintigraphy and positron emission tomography/computed tomography (PET-CT), are better in identifying the majority of lesions and are more ac-

curate in mapping-out the disease.¹⁹ Isolated or common bone pain is the most frequent symptom of ECD.²⁰ Tc-99m MDP scintigraphy showed typical bone lesions affecting the appendicular skeleton consisting of the femur, tibia and fibula and less frequently the ulna, radius and humerus in the four cases we reported. The axial skeleton was generally spared, except for the fact that mandible involvement occurred in all of the cases and maxilla involvement occurred in one case. Scintigraphic changes are considered identifying characteristics for ECD.^{17,18,21} Regional X-Ray, CT or MR imaging performed according to pain localization reveals cortical osteosclerosis, thickening, and bone marrow edema in the long bones. Accompanied by these radiological findings, some diseases including osteomyelitis, lymphoma, sarcoidosis, Paget's disease, metabolic disorders and metastases should be considered in the differential diagnosis.^{22,23} One of the patients we reported was initially admitted and treated for osteomyelitis according to both radiological and histopathological diagnosis. However, typical bone findings in the Tc-99m MDP scintigraphy which was performed in the follow-up, suggested a diagnosis of ECD and aided in the

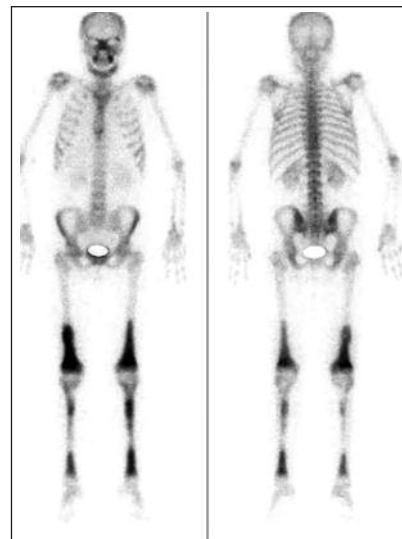


FIGURE 7: Tc-99m MDP scan of a 40-year-old woman with Erdheim-Chester disease (Case 4). The scan revealed patchy increased activity uptake bilaterally in the femur and tibiae, more frequently in the metaphyseal-diaphyseal regions, spreading the epiphyseal portions of the knee and ankle periphery long bones, and diffuse increased activity uptake in the whole side of the mandible.

differential diagnosis of other diseases. Immunohistopathological reevaluation of the bone biopsy verified the scintigraphic diagnosis as ECD.

Various internal organ involvements have been reported in the literature including the hypophysis, lung and the kidneys, indicating disseminated histiocytic infiltration of ECD.²⁴⁻²⁶ Therefore, assessment of the presence of visceral involvement using the best imaging technique is an important matter. FDG PET/CT has better resolution and is considered superior in the evaluation of the extent of both skeletal and extraskelatal disease simultaneously. Two of our patients underwent FDG PET/CT and different soft tissue involvements were observed in them. In one patient, in addition to skeletal system findings, hypophyseal and testicular involvements were noticed through FDG PET/CT. The pituitary gland lesion had already been shown by cerebral MR and infiltration of ECD was verified with histopathological analysis. In addition, bilateral intense FDG uptake was noteworthy in the testicular parenchymas. However, due to bilateral diffuse infiltration, no lobar or nodular pathologies could be detected on ultrasonography and CT. The value of these imaging modalities seems to be limited in those with diffuse tissue infiltration.²⁷ There have been a few case reports in the literature regarding the testicular infiltration of ECD.^{9,26,28} To our knowledge, this is the first time that ECD involvement of the testicular parenchymas has been described by FDG PET/CT.

A pathogenic BRAF (V600E) mutation was detected in the paraffin blocks of the pituitary gland lesion of our patient in whom hypophyseal and testicular involvements were detected. A study reported by Yun et al. found that in colorectal cancer cell lines, the increase of GLUT1 expression and glucose uptake is substantially related to BRAF mutation.²⁹ In these cell lines, it was shown that BRAF mutation up-regulated GLUT1 expression and this led to an increase in glucose uptake of 2.0 to 3.0 fold and in SUVmax of 1.5 to 1.7 fold. A pathogenic BRAF (V600E) mutation was detected in the paraffin blocks of the pituitary gland lesion of our patient in whom hypophyseal and testicular involvements were detected. In the other three

ECD patients, testing for BRAF was not performed. The results of BRAF mutation analysis and FDG PET/CT scan could probably be compared with further studies in the larger number of ECD patients.

As well as in neuroendocrine tumors, somatostatin receptors have been found to be over expressed in miscellaneous tumors and diseases such as thyroid cancer, small cell lung cancer, breast cancer, prostate cancer, and Von Hippel Lindau Disease.^{30,31} Moreover, somatostatin analogues have been radiolabeled with gamma emitters and positron emitters.³² With the introduction of different PET radiopharmaceuticals involving peptide receptor, further developments have occurred in the diagnosis and treatment of the above diseases. Currently, somatostatin analogs labeled with Ga-68 are attracting interest to determine the receptor affinity profiles and to detect more lesions in a wider range of tumors.

Although Ga-67 citrate imaging of a few cases with ECD has been reported in the literature, the somatostatin receptor expression status of the disease has not been described so far.^{16,33,34} In terms of additional diagnostic information and guiding further management, Ga-68 DOTA-TATE imaging was performed in one of our patients. Both F-18 FDG and Ga-68 DOTA-TATE PET/CT images revealed a similar apparent related to bone and soft tissue involvements. However, as there was a mild and moderately uptake of the Ga-68 DOTA-TATE in all lesions, the patient was supposed not to be a good candidate for peptide receptor radionuclide therapy.

In another patient who underwent FDG PET/CT, the presence of liver and lymph node involvements, which have rarely been reported in the literature, was seen in addition to the skeletal system findings.^{8,35-37}

The axial fusion sections of the PET/CT imaging showed inhomogeneous, moderate and intense FDG uptake located in the subcapsular regions of the highly enlarged liver. Diagnostic CT imaging was previously performed for evaluation of the abdomen revealed a homogeneous density pattern

with uniform enhancement, and therefore was unable to show liver involvement. Nevertheless, the main advantage of functional imaging methods over ultrasonography, CT and MR, is their ability to determine metabolic changes before the structural changes become conspicuous.³⁸

In conclusion, as the number of cases described in the literature increases, the awareness of physicians will result in an increase in ECD diagnoses. Having knowledge of the characteristic clinical and imaging manifestations may provide a consensus in the early stage of the disease and an accurate approach for the management of ECD. In this rare but intractable form of histiocytosis, sometimes biopsy materials and immunohistochemical analyses may be inconclusive for diagnosis. Therefore, knowledge of the distinctive imaging findings and clinical manifestations of this condition may help to achieve a correct diagnosis.

Our recommendation is that clinicians should utilize nuclear medicine techniques more. At the same time, nuclear medicine physicians should also increase their expertise to recognize the disease whether histopathological diagnosis is present or not. Bone lesions, nearly always present in ECD, are best visualized by Tc-99m MDP scintigraphy. To obtain an exact mapping-out of the disease with osseous and extraosseous manifestations, F-18 FDG PET/CT is an exceptional method to strengthen the clinician's hand. Additionally, Ga-68 somatostatin receptor imaging may also be a useful tool for determining the receptor affinity profiles and the extent of ECD. Furthermore, by means of comparative studies with BRAF mutation testing, research is required to determine whether FDG PET/CT scan might have a predictive value in the prognosis and therapy management of ECD patients.

REFERENCES

- Chester W. Uber lipidgranulomatose (over lipid granulomatosis). *Virchows Arch Pathol Anat Physiol* 1930;279:561-602.
- Jaffe HL. *Metabolic, Degenerative and Inflammatory Disease of Bone and Joints*. Urban and Schwarzenberg. Munchen-Berlin-Wien; 1972.
- Veyssier-Belot C, Cacoub P, Caparros-Lefebvre D, Wechsler J, Brun B, Remy M, et al. Erdheim-Chester disease. Clinical and radiologic characteristics of 59 cases. *Medicine (Baltimore)* 1996;75(3):157-69.
- Tran TA, Fabre M, Pariente D, Craiu I, Haroche J, Charlotte F, et al. Erdheim-Chester disease in childhood: a challenging diagnosis and treatment. *J Pediatr Hematol Oncol* 2009;31(10):782-6.
- Song SY, Lee SW, Ryu KH, Sung SH. Erdheim-Chester disease with multisystem involvement in a 4-year-old. *Pediatr Radiol* 2011;42(5):632-5.
- Lauretta L, Dagna L, Alberti L, Loiacono F, De Cobelli F, Sanvito F, et al. [Cardiovascular involvement in Erdheim-Chester syndrome: clinical and therapeutic implications]. *Recenti Prog Med* 2013;104(12):637-42.
- Ahuja J, Kanne JP, Meyer CA, Pipavath SN, Schmidt RA, Swanson JO, et al. Histiocytic disorders of the chest: imaging findings. *Radiographics* 2015;35(2):357-70.
- Lim J, Kim KH, Suh KJ, Yoh KA, Moon JY, Kim JE, et al. A Unique case of Erdheim-Chester disease with axial skeleton, lymph node, and bone marrow involvement. *Cancer Res Treat* 2016;48(1):415-21.
- Sheu SY, Wenzel RR, Kersting C, Merten R, Otterbach F, Schmid KW. Erdheim-Chester disease: case report with multisystemic manifestations including testes, thyroid, and lymph nodes, and a review of literature. *J Clin Pathol* 2004;57(11):1225-8.
- Perez A, Crahes M, Laquerrière A, Proust F, Derrey S. Neurological form of Erdheim-Chester disease: case report and review of the literature. *Neurochirurgie* 2014;60(6):316-20.
- Viswanathan S, Kadir NA, Lip AC, Rafia MH. Central nervous system Erdheim Chester disease presenting with raised intracranial pressure and cerebellar signs mimicking neurosarcooidosis with secondary cerebral venous thrombosis. *Neurol India* 2014;62(4):446-8.
- Berti A, Ferrarini M, Ferrero E, Dagna L. Cardiovascular manifestations of Erdheim-Chester disease. *Clin Exp Rheumatol* 2015; 33(2 Suppl 89):S-155-63.
- Balink H, Hemmelder MH, de Graaf W, Grond J. Scintigraphic diagnosis of Erdheim-Chester disease. *J Clin Oncol* 2011;29(16):e470-2.
- Sioka C, Estrada-Veras J, Maric I, Gahl WA, Chen CC. FDG PET images in a patient with Erdheim-Chester disease. *Clin Nucl Med* 2014;39(2):170-7.
- Steňová E, Steňo B, Povinec P, Ondriaš F, Rampalová J. FDG-PET in the Erdheim-Chester disease: its diagnostic and follow-up role. *Rheumatol Int* 2012;32(3):675-8.
- Martin W 3rd, Hoffnung JM, Teague R, Cowan RJ. Gallium uptake in Erdheim-Chester disease. *Clin Nucl Med* 1982;7(10):468.
- Franzius C, Sciuk J, Bremer C, Kempkes M, Schober O. Determination of extent and activity with radionuclide imaging in Erdheim-Chester disease. *Clin Nucl Med* 1999; 24(4):252-5.
- Mukherjee A, Damle N, Bal C, Arora A, Singhal A, Tripathi M, et al. Role of (99m)Tc-MDP bone scan in the diagnosis of Erdheim-Chester disease. *Indian J Nucl Med* 2014; 29(3):165-7.
- Antunes C, Graça B, Donato P. Thoracic, abdominal and musculoskeletal involvement in Erdheim-Chester disease: CT, MR and PET imaging findings. *Insights Imaging* 2014;5(4): 473-82.
- Lu T, Cao X, Luo Y, Cai H, Zhang W, Zhong D. [Clinical and pathologic characteristics of Erdheim-Chester disease]. *Zhonghua Bing Li Xue Za Zhi* 2014;43(12):809-13.

21. De Filippo M, Ingegnoli A, Carloni A, Verardo E, Sverzellati N, Onniboni M, et al. Erdheim-Chester disease: clinical and radiological findings. *Radiol Med* 2009;114(8):1319-29.
22. Guo S, Yan Q, Rohr J, Wang Y, Fan L, Wang Z. Erdheim-Chester disease involving the breast--a rare but important differential diagnosis. *Hum Pathol* 2015;46(1):159-64.
23. Ihde LL, Forrester DM, Gottsegen CJ, Masih S, Patel DB, Vachon LA, et al. Sclerosing bone dysplasias: review and differentiation from other causes of osteosclerosis. *Radiographics* 2011;31(7):1865-82.
24. Manaka K, Makita N, Iiri T. Erdheim-Chester disease and pituitary involvement: a unique case and the literature. *Endocr J* 2014; 61(2):185-94.
25. Arnaud L, Pierre I, Beigelman-Aubry C, Capron F, Brun AL, Rigolet A, et al. Pulmonary involvement in Erdheim-Chester disease: a single-center study of thirty-four patients and a review of the literature. *Arthritis Rheum* 2010;62(11):3504-12.
26. Yelfimov DA, Lightner DJ, Tollefson MK. Urologic manifestations of Erdheim-Chester disease. *Urology* 2014;84(1):218-21.
27. Sachpekidis C, Mai EK, Goldschmidt H, Hillengass J, Hose D, Pan L, et al. (18)F-FDG dynamic PET/CT in patients with multiple myeloma: patterns of tracer uptake and correlation with bone marrow plasma cell infiltration rate. *Clin Nucl Med* 2015;40(6):e300-7.
28. Juanós Iborra M, Selva-O'Callaghan A, Solanich Moreno J, Vidaller-Palacin A, Martí S, Grau Junyent JM, et al; Grupo para estudio de la Enfermedad de Erdheim-Chester. [Erdheim-Chester disease: study of 12 cases]. *Med Clin (Barc)* 2012;139(9):398-403.
29. Yun J, Rago C, Cheong I, Pagliarini R, Angenendt P, Rajagopalan H, et al. Glucose deprivation contributes to the development of KRAS pathway mutations in tumor cells. *Science* 2009;325(5947):1555-9.
30. Reubi JC. Peptide receptors as molecular targets for cancer diagnosis and therapy. *Endocr Rev* 2003;24(4):389-427.
31. Oh JR, Kulkarni H, Carreras C, Schalch G, Min JJ, Baum RP. Ga-68 somatostatin receptor PET/CT in von Hippel-Lindau disease. *Nucl Med Mol Imaging* 2012;46(2):129-33.
32. Antunes P, Ginj M, Zhang H, Waser B, Baum RP, Reubi JC, et al. Are radiogallium-labelled DOTA-conjugated somatostatin analogues superior to those labelled with other radiometals? *Eur J Nucl Med Mol Imaging* 2007;34(7): 982-93.
33. Kudo Y, Iguchi N, Sumiyoshi T, Murai T, Oka T. Dramatic change of Ga-67 citrate uptake before and after corticosteroid therapy in a case of cardiac histiocytosis (Erdheim-Chester disease). *J Nucl Cardiol* 2006;13(6):867-9.
34. Sohn MH, Kim MW, Kang YH, Jeong HJ. Tc-99m MDP bone and Ga-67 citrate scintigraphy of Erdheim-Chester disease in a child. *Clin Nucl Med* 2006;31(2):90-2.
35. Gupta A, Aman K, Al-Babtain M, Al-Wazzan H, Morouf R. Multisystem Erdheim-Chester disease; a unique presentation with liver and axial skeletal involvement. *Br J Haematol* 2007;138(3):280.
36. Tsynman DN, Weaver C, Taboada S, Findeis-Hosey J, Maliakkal B, Huang J. Portal hypertension and ascites secondary to Erdheim Chester disease without intrinsic liver involvement on liver biopsy. *Dig Liver Dis* 2013; 45(11):964-5.
37. Ivan D, Neto A, Lemos L, Gupta A. Erdheim-Chester disease: a unique presentation with liver involvement and vertebral osteolytic lesions. *Arch Pathol Lab Med* 2003;127(8): e337-9.
38. D'souza MM, Jaimini A, Bansal A, Tripathi M, Sharma R, Mondal A, et al. FDG-PET/CT in lymphoma. *Indian J Radiol Imaging* 2013; 23(4):354-65.